Supporting Information

Lacroix et al. 10.1073/pnas.1010167107

SI Materials and Methods

Generation of *E4F1*$^{-/flox}$ and Compound Mice. The E4F1 targeting construct was generated by cloning *129/SvJ* murine genomic *E4F1* sequences (1) into the pDT915 targeting vector. Lox-P sites were introduced before exon 4 and after exon 14, as shown in Fig. S1. A hygromycin-TK cassette flanked by two FRT sequences was added after the polyA signal of the *E4F1* gene. The targeting vector was linearized by NotI and electroporated in J1 ES cells (*129/SvJ*). The latter were selected with hygromycin B (130 μg/mL; Calbiochem) for 1 wk before clonal amplification. Correct targeting of the *E4F1* locus was assessed on genomic DNA prepared from hygromycin-resistant ES clones by Southern blot analysis using probes corresponding to 5′ (400 bp) and 3′ (360 bp) flanking sequences of the E4F1 gene (Fig. S1). Targeted ES cells were electroporated with a flippase-expressing vector (a gift of Dr. S. Dymecki, Harvard Medical School, Boston) and selected using ganciclovir (4 μM) to enrich for clones in which the hygromycin-TK cassette was deleted. Several *E4F1*$^{+/flox}$ ES clones displaying a normal karyotype were subsequently injected into *C57BL/6* blastocysts. Chimeric mice were mated with *C57BL/6* mice for germline transmission of the E4F1 flox allele. Heterozygous mutant mice *E4F1*$^{+/flox}$ and *E4F1*$^{+/-}$ were interbred to generate *E4F1*$^{-/flox}$ animals. *E4F1* recombination was assessed by immunoblot analysis or by quantitative PCR analysis on skin genomic DNA using primers specific for the *E4F1* locus, as shown in Fig. S1 *C–E* (primer A: 5′-GGCTGCTGCGTGGATTTC; primer B: 5′-GCTAGGTAGGGTAGGAGGCTGTCT; primer C: 5′-ACC-GGCGTGTTCACTCAGAC; primer D: 5′-GCAGAACTGG-CACACGTGG; primer E: 5′-TTCGGTATAGTGTTGAGG; primer F: 5′-AGGGGCTGGGCTACAATGG).

E4F1$^{-/flox}$ mice were crossed with *Cre-ER*^{T2} knock-in mice (*RERT*) (2) or *K5-Cre* transgenic mice (3) to obtain *E4F1*$^{-/flox}$;*RERT*$^{KI/KI}$ and *E4F1*$^{-/flox}$;*K5-Cre* mice, respectively. *E4F1*^{flox};*RERT* mice also were crossed with *K15-EGFP* transgenic mice (Jackson Laboratory) (4) to generate *E4F1*^{flox};*RERT*$^{KI/KI}$;*K15-GFP* mice and with *Ink4a/Arf*$^{-/-}$ mice (5) to generate *E4F1*^{flox};*RERT*$^{KI/KI}$;*Ink4a/Arf*$^{-/-}$ mice.

Genotyping. *E4F1*^{flox};*RERT* mice were genotyped by PCR on tail genomic DNA using the following primers: (*i*) E4F1 WT (*E4F1*$^{+}$) and conditional KO flox alleles (*E4F1*^{flox}): 5′-CCTTGAGCA-CGGAGGAGAGC-3′ and 5′-GCCCTAGCCTGCTC-TGCCA-TC-3′; (*ii*) *E4F1* constitutive KO allele (*E4F1*$^{-}$): 5′-CACTGC-CTTGGAGGACTTTG-3′ and 5′-CCTCTGTTCCACA-TACA-CTTCATTC-3′; (*iii*) WT and knock-in *RERT* alleles: 5′-GTCAG-TACACATACAGACTT-3′, 5′-TGAGCGAACAGGGCGAA-3′, and 5′-TCCATGGAGCACCCAGTGAA-3′; (*iv*) *K5-Cre* transgene: 5′-AACATGCTTCATCGTCGG-3′ and 5′-TTCGG-ATCATCAGCTACACC-3′; (*v*) *K15-GFP* transgene: 5′-CTA-CGGCGTGCAGTGCTTCAGC-3′ and 5′-GGCGAGCTGCA-CGCTGCGTCCTC-3′; and (*vi*) *Ink4a/Arf* alleles: WT, 5′-AT-GATGATGGGCAACGTTC-3′ and 5′-CAAATATCGCACG-ATGTC-3′; KO, 5′-CTATCAGGACATAGCGTTGG-3′ and 5′-AGTGAGAGTTTGGGGACAGAG-3′.

Histochemistry and Immunolabeling of Skin Sections and Whole Mounts. Skin biopsy specimens were either fixed in 4% neutral-buffered formalin (24 h) and paraffin-embedded or frozen in Tissue-Tek OCT Compound (Sakura) for cryosectioning. Paraffin-embedded tissues were sectioned and processed for IHC or H&E staining. IHC was performed on 4-μm sections using appropriate primary antibodies: anti-E4F1 (B-21 rabbit polyclonal, generated by our laboratory), anti-Ki67 (SP6; Neomarkers), anti-K6 (SPM269; Abcam), anti-K10 (PRB-159P; Covance), anti-involucrin (Sc15230; Santa Cruz Biotechnology), anti-CD34 (RAM34; BD Pharmingen), and anti-K15 (LHK15; Vector Laboratories). All secondary antibodies were diluted at 1:200 in biotinylated secondary antibody coupled to streptavidin–peroxidase complex (ABC Vectastain Kit; Vector Laboratories). Revelation was performed using the peroxidase substrate DAB (Vector Laboratories). Immunohistofluorescence staining with anti–α6-integrin (GoH3; BD Biosciences) and anti-K14 (AF64; Covance) were performed on 10-μm cryosections fixed for 10 min in 100% acetone. Secondary alexa-conjugated antibodies were diluted at 1:1,000 for immunohistofluorescence (Invitrogen).

Apoptotic cells were detected using a TUNEL staining kit (Roche) or by IHC with anti–caspase 3 antibody. For morphological analysis of sebaceous glands, whole mounts of tail epidermis were stained with Nile red (0.1 mg/mL; Sigma-Aldrich) for 30 min at room temperature.

BrdU-positive cells were detected using anti-BrdU antibody (BD Biosciences). Whole mounts of tail epidermis and detection of LRCs were prepared as described previously (6), and pictures were generated using a Zeiss 510 confocal microscope and presented as Z-stack projections after deconvolution with Imaris software (Bitplane).

Culture of Primary Keratinocytes and Clonogenic Assays. Murine primary keratinocytes were isolated from newborn skin after overnight treatment with dispase (5 mg/mL; Roche) or from adult back skin after overnight treatment with trypsin-EDTA, and were grown in calcium-free Eagle's minimal essential medium (Bio-Whittaker; Lonza) containing 10% calcium-free FCS (Sigma-Aldrich) and 10 μg/mL of murine EGF (Roche). Cre-mediated recombination of *E4F1 flox* alleles was achieved by adding 4OHT (1 μM; Sigma-Aldrich) to the culture medium. Human primary keratinocytes were isolated from skin biopsy specimens obtained after medical surgery and cultured in Green medium containing 1.2 mM calcium as described previously (7) and in accordance with the Declaration of Helsinki.

For cell cycle analyses, BrdU (10 mM; Sigma-Aldrich) was added for 24 h in the culture medium supplemented with 10% or 2% FCS. For clonogenic assays, 2,000–10,000 total primary keratinocytes per well were plated on a confluent feeder layer of inactivated J2-3T3 fibroblasts (3 h of treatment with mitomycin C at 4 μg/mL; Sigma-Aldrich) grown on collagen-I–coated six-well plates at 32 °C in 8% CO_2 (mouse keratinocytes) or at 37 °C in 10% CO_2 (human keratinocytes). Clonogenic assays were performed in calcium-free DMEM-HamF12 (3:1) (Invitrogen) containing 10% calcium-free FCS (Sigma-Aldrich), 4 mM L-glutamine, 110 mg/L of Na pyruvate, 8 ng/mL of choleratoxine (Sigma-Aldrich), 0.4 μg/mL of hydrocortisone (Sigma-Aldrich), 5 μg/mL of insulin (Sigma-Aldrich), and 10 μg/mL of murine EGF (Roche). Colonies were fixed with 4% PFA and stained with 1% rhodamine B (Sigma-Aldrich). Quantitative analysis of the total number and size of clones was performed with ImageJ software (National Institutes of Health).

Retroviral and Lentiviral Particle Production and Infections. Retroviral and lentiviral particles were produced in 293T cells by transient transfection using Jet-PEI reagent (Ozyme) of gag/pol, env-VSV-G, and indicated viral constructs pMSCV-Bmi1 (8), pMKO vector encoding either control or antihuman E4F1 shRNAs (sequences available on request), pLKO1 encoding shRNAs directed against murine RB1 or p53 (MISSION shRNA

clones NM_011640.1–625s1c1; Sigma-Aldrich), or control irrelevant sequences. At 48 h after transfection, viral supernatants were harvested and added to primary keratinocytes overnight with polybrene 8 μg/mL (Sigma-Aldrich). Antibiotic selection of transduced primary murine keratinocytes was performed 48 h later with puromycin (1.25 μg/mL; pLKO1), or blasticidin (5 μg/mL; pMSCV).

Western Blot Analyses. Total cell extracts were prepared in 50 mM Tris-HCl (pH 7.4), 100 mM NaCl, 5 mM EDTA, and 0.5% Nonidet P-40, supplemented with protease inhibitors (complete medium; Roche). Immunoblots were probed with primary antibodies directed against E4F1 (9), p53 (1C12; Cell Signaling), Bmi1 (F6; Millipore), $p19^{ARF}$ (Ab80; Abcam), and β-actin (Sigma-Aldrich).

FACScan Analyses. Freshly isolated cell suspensions were incubated with FITC-conjugated anti-CD34 (RAM34; BD Biosciences) and PE-Cy5–conjugated anti–α6-integrin primary antibodies for 30 min at 4 °C. For cell cycle analyses, formalin-fixed cells were incubated with anti-BrdU or anti-phosphoserine 10 histone H3 (6G3 9706; Cell Signaling) and PI (Sigma-Aldrich) as described previously (10). Cells were analyzed on a FACScalibur flow cytometer (BD Biosciences), and data were processed with Flowjo software (Treestar).

Quantitative RT-PCR. Total RNAs were isolated using TriZol reagent (Invitrogen). cDNAs were synthesized from 1 μg of total RNA using random hexamers and SuperScript III reverse transcriptase (Invitrogen). Quantitative real-time PCR was performed on a LightCycler 480 SW 1.5 apparatus (Roche). The *RPL13A* transcript was used for normalization. Primer sequences were as follows: *RPL13A* forward, 5′-GAGGTCGGGTGGAAGTACCA-3′; *RPL13A* reverse, 5′-TGCATCTTGGCCTTTTCCTT-3′; *p16* forward, 5′-GTACCCCGATTCAGGTGATG-3′; *p16* reverse, 5′-GGAGAAGGTAGTGGGGTCCT-3′; *p19* forward, 5′-CCCACTCCAAGAGAGGTTTT-3′; *p19* reverse, 5′-ATGTTCACGAAAGCCAGAGC-3′; *Notch1* forward, 5′-CTTCGTGCTCCTGTTCTTTGT-3′; *Notch1* reverse, 5′- GGTGCGGTCTGTCTGGTTGTG-3′, *ΔNp63* forward, 5′-ATGTTGTACCTGGAAAACAATG 3′; *ΔNp63* reverse, 5′-GATGGAGAGAGGGCATCAAA-3′; *Perp* forward, 5′-CCCAGATGCTTGTTTTCCTG-3′; *Perp* reverse, 5′-ACCAGGGAGATGATCTGGAAT-3′; *Claudin-1* forward, 5′-ACTCCTTGCTGAATCTGAACAGT-3′; *Claudin-1* reverse, 5′-GGACACAAAGATTGCGATCAG-3′; *Fibronectin1* forward, 5′-TGAAGTCGCAAGGAAACAAGC-3′; *Fibronectin1* reverse, 5′-TGAACGGGAGGACACAGGG-3′; *EVA1* forward, 5′-GTGGGAGATGCGCTAACTGT-3′; *EVA1* reverse, 5′-TGTCCCATTGTCGTCAAACT-3′; *Runx1* forward, 5′-CGAAGACATCGGCAGAAACT-3′; *Runx1* reverse, 5′-GGCATCCTGCATCTGACTTT-3′; *Redd1* forward, 5′-ACTCTTCCTTGGTCCCTGGT-3′; and *Redd1* reverse, 5′-CAGGGGACAGTCCTTCAGTC-3′.

1. Le Cam L, Lacroix M, Ciemerych MA, Sardet C, Sicinski P (2004) The E4F protein is required for mitotic progression during embryonic cell cycles. *Mol Cell Biol* 24:6467–6475.
2. Guerra C, et al. (2003) Tumor induction by an endogenous *K-ras* oncogene is highly dependent on cellular context. *Cancer Cell* 4:111–120.
3. Ramirez A, et al. (2004) A keratin K5Cre transgenic line appropriate for tissue-specific or generalized Cre-mediated recombination. *Genesis* 39:52–57.
4. Morris RJ, et al. (2004) Capturing and profiling adult hair follicle stem cells. *Nat Biotechnol* 22:411–417.
5. Serrano M, et al. (1996) Role of the *INK4a* locus in tumor suppression and cell mortality. *Cell* 85:27–37.
6. Braun KM, et al. (2003) Manipulation of stem cell proliferation and lineage commitment: Visualisation of label-retaining cells in whole mounts of mouse epidermis. *Development* 130:5241–5255.
7. Bitoun E, et al. (2003) LEKTI proteolytic processing in human primary keratinocytes, tissue distribution and defective expression in Netherton syndrome. *Hum Mol Genet* 12:2417–2430.
8. Jacobs JJ, Kieboom K, Marino S, DePinho RA, van Lohuizen M (1999) The oncogene and Polycomb-group gene *bmi-1* regulates cell proliferation and senescence through the *ink4a* locus. *Nature* 397:164–168.
9. Fajas L, et al. (2000) pRB binds to and modulates the transrepressing activity of the E1A-regulated transcription factor $p120^{E4F}$. *Proc Natl Acad Sci USA* 97:7738–7743.
10. Le Cam L, et al. (2006) E4F1 is an atypical ubiquitin ligase that modulates p53 effector functions independently of degradation. *Cell* 127:775–788.

Fig. S1. Generation and validation of *E4F1* conditional KO mice. (*A*) Schematic representation of the unmodified (*Top*), targeting vector (*Middle*), and recombined *E4F1 flox* allele (*Bottom*). (*B*) Homologous recombination was verified on both ends by Southern blot analysis using 5′ (*Left*) and 3′ (*Right*) external probes. (*C*) (*Upper*) The hygromycin-thymidine kinase (*Hygro-TK*) resistance cassette was removed in vitro after a second round of electroporation of homologous recombinant ES clones using Flpe recombinase. (*Lower*) Schematic representation of the floxed E4F1 allele after Cre-mediated recombination. (*D*) Cre-mediated recombination of the $E4F1^{flox}$ allele in skin. Quantitative (*Left*) or semiquantitative (*Right*) PCR analyses were performed on genomic DNA extracted from back skin of $E4F1^{+/-}$ or $E4F1^{-/flox}$;*RERT* adult mice after topical application of 4OHT or from back skin of $E4F1^{+/-}$ or $E4F1^{-/flox}$;*K5-Cre* P1 neonates. The primer pairs used for PCR amplification are indicated by arrows in *C*. Note that primer pair A/B generates a PCR amplicon only after Cre-mediated recombination. Normalization for equal amounts of genomic DNA in those assays was controlled with primers (E/F) located in the nonrecombined region of the *E4F1* locus. (*E*) Immunoblots showing E4F1 expression after Cre-mediated recombination in primary keratinocytes isolated from $E4F1^{flox}$;*RERT* and treated with 4OHT (*Left*) or from $E4F1^{flox}$;*K5* neonatal epidermis (*Right*). ns, nonspecific signal.

Fig. S2. *E4F1* inactivation results in hyperproliferation of epidermal cells. Immunofluorescent images of dorsal skin sections prepared from 4OHT-treated $E4F1^{flox}$;*RERT* adult mice injected with BrdU (for 4 h), immunostained with anti-BrdU (red) antibody, and costained with DAPI (blue). The dashed line indicates the basal membrane and the interface between epidermis (*Upper*) and dermis (*Lower*). (Scale bar: 50 μm.) The genotype of the analyzed mice is indicated. The histogram quantifies the percentage of BrdU-positive cells in a representative experiment.

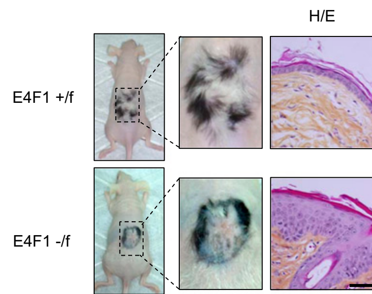

Fig. S3. *E4F1* inactivation results in skin autonomous effects in the RERT model. Back skin from *E4F1*$^{+/flox}$*;RERT* or *E4F1*$^{-/flox}$*;RERT* P1 neonates was engrafted onto recipient nude mice and treated with 4OHT. Photographs at low (*Left*) or higher (*Middle*) magnification of representative engrafted skin were taken at 2 wk after *E4F1* inactivation. (*Right*) H&E-stained sections of engrafted skin showing hyperplasia of *E4F1*-depleted epidermis. (Scale bar: 40 μm.)

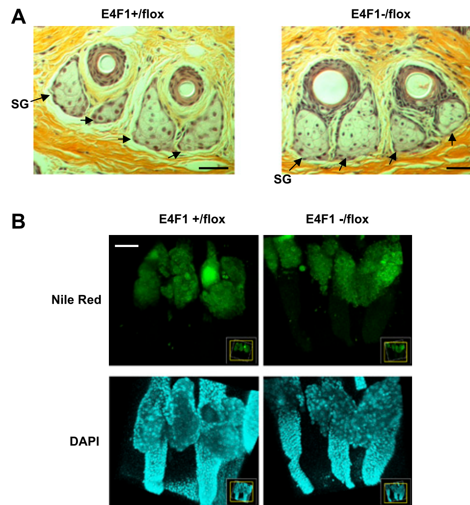

Fig. S4. Sebaceous glands appear to be unaltered after *E4F1* inactivation. (*A*) H&E staining of tail skin cross-sections from *E4F1*$^{+/flox}$ and *E4F1*$^{-/flox}$*;RERT* at 6 wk after *E4F1* inactivation. Arrows indicate sebaceous glands (SG). (*B*) Nile red (green) staining of sebaceous glands in whole mounts of tail epidermis prepared from *E4F1*$^{+/flox}$ and *E4F1*$^{-/flox}$*;RERT* mice at 6 wk after 4OHT application. DAPI staining (blue) shows general morphology. (Scale bar: 100 μm.)

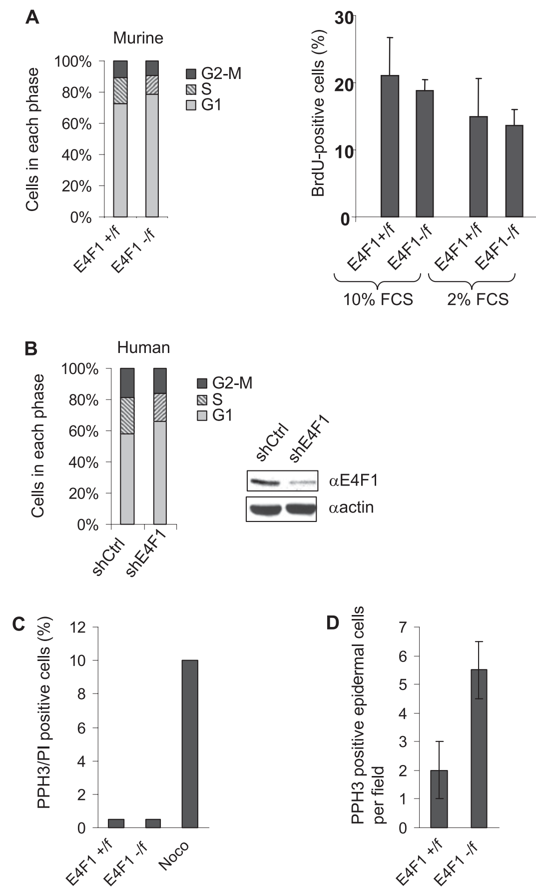

Fig. S5. *E4F1* inactivation does not enhance the short-term proliferation of primary keratinocytes in culture. (*A*) *E4F1* inactivation in vitro does not result in murine keratinocyte hyperproliferation. (*Left*) Cell cycle profiles of murine *E4F1*$^{+/flox}$ or *E4F1*$^{-/flox}$*;K5-Cre*. The percentage of cells in each phase of the cell cycle was determined by FACScan analysis after costaining with PI and BrdU. (*Right*) This absence of hyperproliferation in *E4F1* KO also was observed when cells were cultured in low-serum medium (containing 2% FCS instead of 10% FCS). (*B*) *E4F1* depletion in vitro does not result in human keratinocyte hyperproliferation. Shown are PI/BrdU costaining profiles of human primary keratinocytes transduced with retroviral vectors expressing either a shRNA targeting human E4F1 (shE4F1) or a control shRNA (shCtrl). (*Right*) Western blot analysis of total protein extracts showing efficient E4F1 depletion. (*C*) Anti-phosphohistone H3/PI labeling and FACScan analyses of murine *E4F1*$^{+/flox}$ or *E4F1*$^{-/flox}$*;RERT* primary keratinocytes after 5 d of culture in the presence of 4OHT. Nocodazole-treated cells (Noco, 10 μM) were used as positive controls. (*D*) IHC analysis of dorsal skin sections from *E4F1*$^{+/flox}$ or *E4F1*$^{-/flox}$*;K5-Cre* P1 neonates with anti–phosphohistone H3 antibody. The number of PPH3-positive cells per field is indicated.

Fig. S6. *E4F1* inactivation results in expansion of the basal cell compartment of the epidermis and abnormal keratinocyte differentiation. (*A*) *E4F1* inactivation results in hyperproliferation of K14- and α6-integrin–positive basal/TAC cells. Immunostaining of dorsal skin cryosections from *E4F1*$^{+/flox}$ and *E4F1*$^{-/flox}$*;RERT* mice with anti-K14 and anti-α6 integrin (α6) antibodies. (Scale bar: 40 μm.) (*B*) IHC analysis of dorsal skin sections from *E4F1*$^{+/flox}$ and *E4F1*$^{-/flox}$*;RERT* mice with anti-K6, anti-K10, or anti-involucrin (invol) antibodies. (Scale bar: 40 μm.)

Fig. S7. (*A*) *E4F1* inactivation results in loss of K15 stem cell marker expression. Immunostaining of HF with anti-K15 (red) in whole mounts of tail epidermis prepared from *E4F1*$^{-/flox}$*;RERT* and control mice at 6 wk after 4OHT application. (*Inset*) The same HFs after anti–integrin-α6 (α6, green) and DAPI costaining (blue) showing general morphology. The HF K15-positive bulge region is indicated by a white bracket. (Scale bar: 50 μm.) (*B*) *E4F1* inactivation triggers hyperproliferation of LRCs. Shown are analyses of BrdU-labeled LRCs (green) and proliferative cells (Ki67, red) in whole mounts of tail epidermis prepared from *E4F1*$^{-/flox}$*;RERT* mice at 2 wk after 4OHT application. The lower-magnification image of the same HFs after DAPI staining (blue) shows general morphology. BrdU and Ki67 double-positive HF LRC stem cells are indicated by white arrows. (Scale bar: 50 μm.)

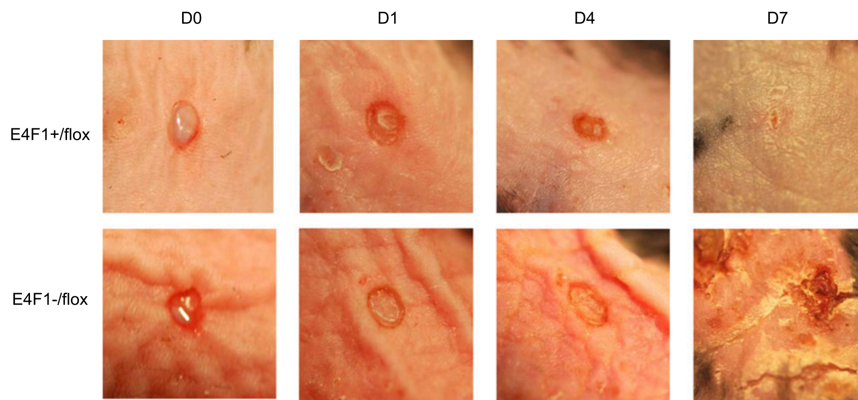

Fig. S8. *E4F1* inactivation alters wound healing. A 5-mm full-thickness punch biopsy was made on the back skin of *E4F1*$^{+/flox}$ and *E4F1*$^{-/flox}$;*RERT* mice treated with 4OHT 3 d earlier. Wound closure was observed at the indicated time points (0, 1, 4, and 7 d after wounding).

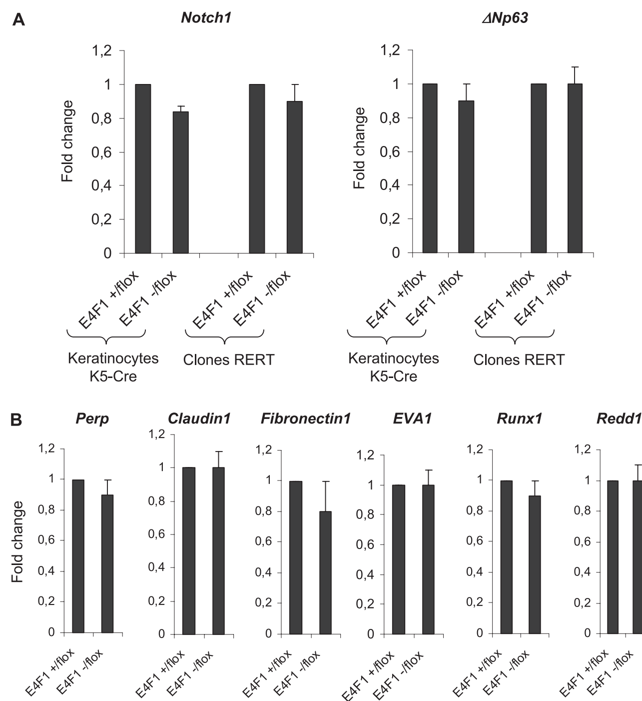

Fig. S9. Transcript levels of *Notch1*, *ΔNp63*, and several p63 target genes are unchanged in *E4F1* KO keratinocytes. (*A*) Quantitative RT-PCR analyses of *Notch1* and *ΔNp63* mRNA levels in keratinocytes isolated from *E4F1*$^{+/flox}$ and *E4F1*$^{-/flox}$;*K5-Cre* neonate skin or from clones established from *E4F1*$^{+/flox}$ and *E4F1*$^{-/flox}$;*RERT* mice treated with 4OHT in vitro. (*B*) Quantitative RT-PCR analyses of several p63 transcriptional target genes (*Perp*, *Claudin1*, *Fibronectin1*, *EVA1*, *Runx1*, and *Redd1*) in keratinocytes isolated from *E4F1*$^{+/flox}$ and *E4F1*$^{-/flox}$;*K5-Cre* neonate skin.